

Supporting Information

Highly sensitive and wearable gel-based sensors with dynamic physically cross-linked structure for strain-stimulus detection over a wide temperature range

Shan Xia^a, Shixin Song^a, Yi Li^{b,*}, and Guanghui Gao^{a,*}

^aPolymeric and Soft Materials Laboratory, School of Chemical Engineering and Advanced Institute of Materials Science, Changchun University of Technology, Changchun 130012, China

^bSchool of Chemical Engineering and Theranostic Macromolecules Research Center, Sungkyunkwan University, Suwon, 16419, Republic of Korea

Corresponding authors: Yi Li and Guanghui Gao

E-mail: cc11liyitc@gmail.com; ghgao@ccut.edu.cn

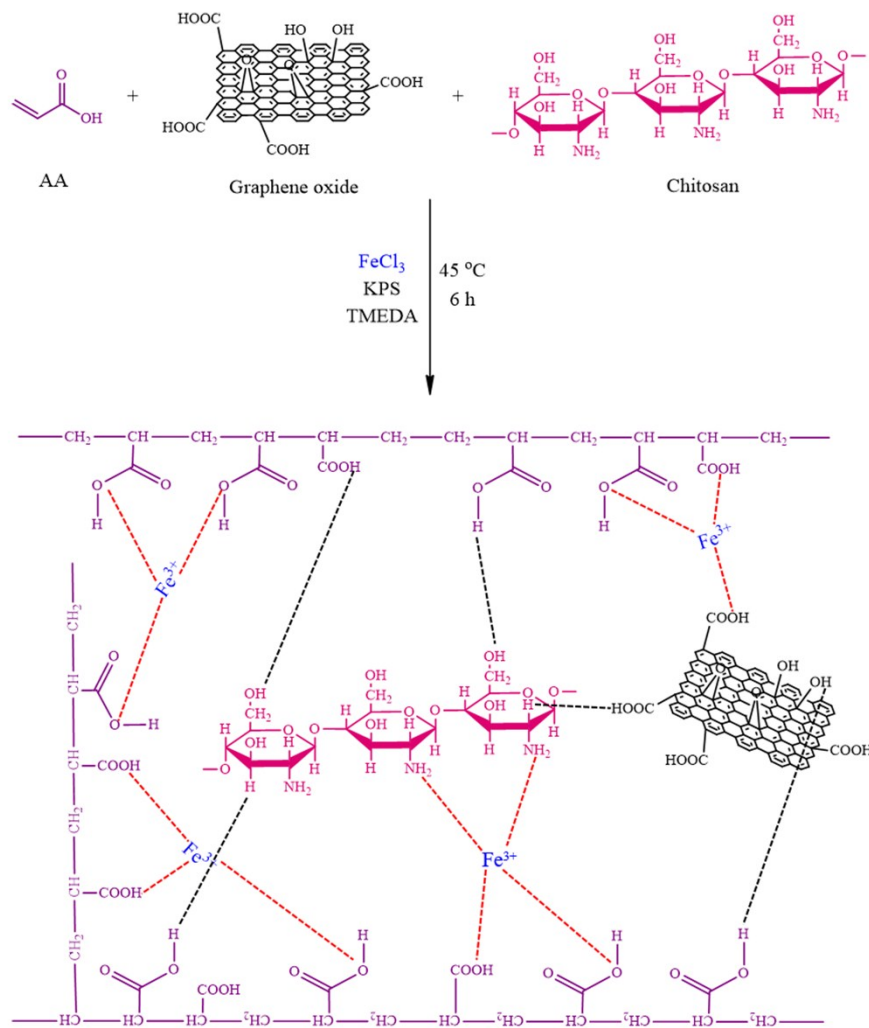


Figure S1. Schematic diagram of the synthesis of PAA/CS/GO/Gly gel network.

The AA, and AA/CS aqueous solution showed no UV absorption. The obvious absorption at 290 nm and 300 nm appeared for FeCl₃ and GO aqueous solution. A weak absorption at 405 nm appeared after AA was mixed with FeCl₃, which demonstrated the Fe³⁺ ions could be coordinated with AA. The UV-Vis of the GO/FeCl₃ aqueous solution was different from that of individual aqueous solution of GO and FeCl₃, suggesting that coordination complex was formed after the reaction between GO and Fe³⁺ ions. Furthermore, the UV-Vis absorption for AA/GO/FeCl₃ aqueous solution was also different from the AA/FeCl₃ and GO/FeCl₃ solutions, which indicated that the AA monomers could be linked to GO by Fe³⁺ ions coordination. And the UV-Vis absorption for AA/CS/GO/FeCl₃ aqueous solution was shifted compared with that of AA/GO/FeCl₃, proved that there was coordination interaction between Fe³⁺ ions, PAA and CS.

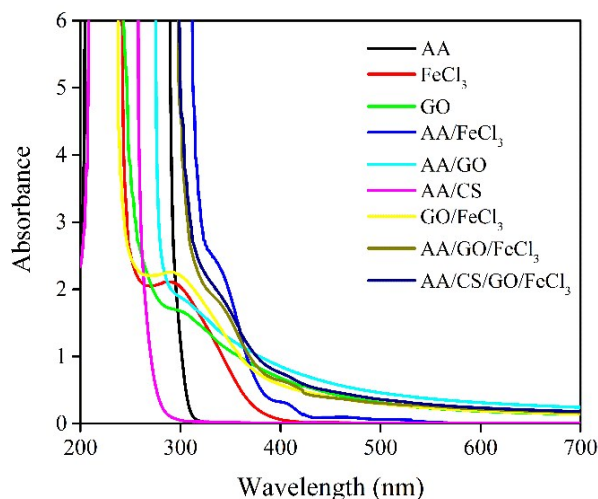


Figure S2. UV-vis spectrums of AA, FeCl₃, GO, AA/FeCl₃, AA/GO, AA/CS, GO/FeCl₃, AA/GO/FeCl₃, AA/CS/GO/FeCl₃ aqueous solutions.

The effect of FeCl₃ contents on the mechanical property of PAA/CS/GO gel was investigated and the result was shown in Figure S3 and Table S1. The tensile strength, toughness and elastic modulus increased considerably with increasing FeCl₃ content due to the increased electrostatic interaction in gels which could effectively dissipate energy by destruction and reformation.

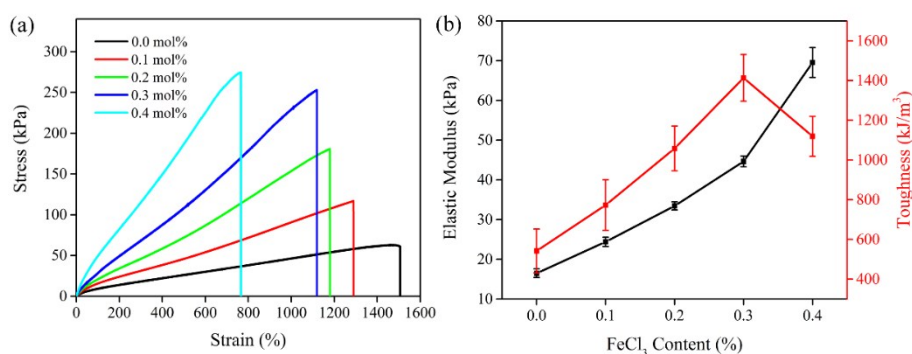


Figure S3. a) tensile curves and b) corresponding the elastic modulus and toughness (fracture energy) from a) of PAA/CS/GO gel with different FeCl₃ contents.

Table S1. Influence of FeCl₃ contents on mechanical properties of gels.

FeCl ₃ Content (mol% to AA)	Elastic Modulus (kPa)	Fracture Stress (kPa)	Fracture Strain (%)	Toughness (kJ/m ³)
0.00	16.5 ± 1.07	63.3 ± 3.74	1507.3 ± 147.2	542.2 ± 120.4
0.25	24.4 ± 1.15	117.3 ± 8.92	1290.3 ± 104.5	773.2 ± 137.4
0.50	33.5 ± 1.03	182.7 ± 15.42	1178.7 ± 100.5	1058.6 ± 112.4
0.75	44.6 ± 1.37	254.8 ± 32.41	1119.6 ± 107.3	1413.9 ± 118.4
1.00	19.6 ± 3.74	275.9 ± 37.54	762.8 ± 86.7	1119.3 ± 101.4

Furthermore, the effect of contents of GO on the mechanical properties of PAA/CS/GO gel was also investigated. As shown in Figure S4 and Table S2, the tensile strength, elastic modulus and toughness increased with increasing GO contents from 0.00 wt% to 0.75 wt%, and then decreased at the GO content of 1.00 wt%. It should be attributed to the increased hydrogen bond cross-linking and electrostatic interaction. However, the increased crosslink density made the network of PAA/CS/GO gel non-uniform, resulting in a decrease in the mechanical properties of the gel. The suitable contents of FeCl₃ and GO were 0.2 mol% and 0.5 wt% to AA monomers.

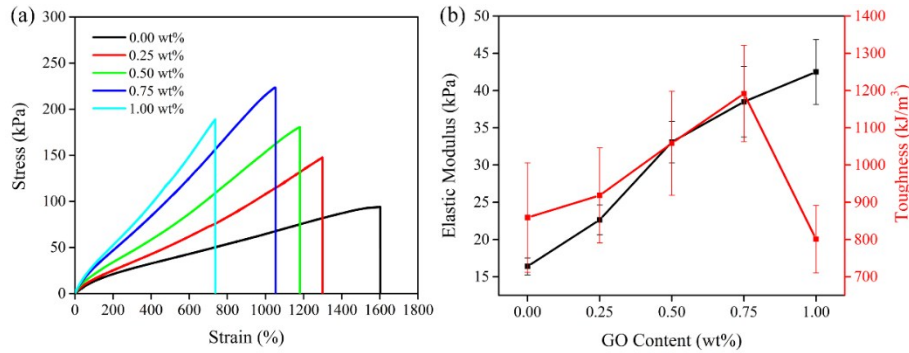


Figure S4. a) tensile curves and b) corresponding elastic modulus and toughness from a) of PAA/CS/GO gels with different GO contents.

Table S2. Influence of GO contents on mechanical properties of PAA/CS/GO gels.

GO Content (wt% to AA)	Elastic Modulus (kPa)	Fracture Stress (kPa)	Fracture Strain (%)	Toughness (kJ/m ³)
0.00	16.4 ± 1.14	95.1 ± 7.24	1601.7 ± 153.4	859.1 ± 147.2
0.25	22.7 ± 1.98	149.2 ± 11.37	1301.4 ± 101.4	918.5 ± 127.6
0.50	33.1 ± 2.79	181.8 ± 13.24	1175.8 ± 93.3	1058.6 ± 139.9
0.75	38.5 ± 4.74	223.6 ± 27.42	1053.5 ± 91.4	1192.1 ± 129.3
1.00	42.5 ± 4.34	189.6 ± 7.94	735.8 ± 121.4	800.9 ± 90.64

Furthermore, the ratio of H₂O and glycerol (Gly) also had obvious effect on the mechanical properties of PAA/CS/GO/Gly gels, as shown in Figure S5 and Table S3. As glycerol content increased, the tensile strength, toughness and elastic modulus increased gradually. This is due to the fact that glycerol could form a large number of hydrogen bonds and the increasing cross-linking could enhance the mechanical property.

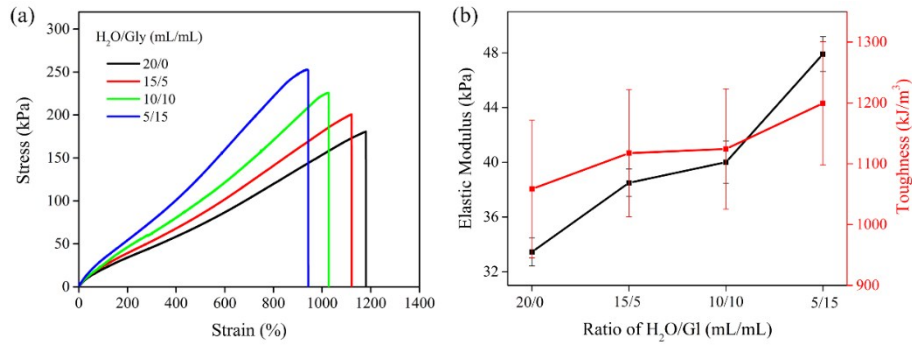


Figure S5. a) tensile curves and b) corresponding fracture stress and strain from a) of PAA/CS/GO/Gly gel with different water contents.

Table S3. Influence of the ratio of H₂O and Gly on mechanical properties of PAA/CS/GO/Gly gel

Ratio of H ₂ O/Gly (mL/mL)	Elastic Modulus (kPa)	Fracture Stress (kPa)	Fracture Strain (%)	Toughness (kJ/m ³)
20/0	33.5 ± 1.03	181.6 ± 11.74	1180.7 ± 90.3	1058.6 ± 113.2
15/5	38.5 ± 1.00	200.8 ± 20.34	1120.7 ± 101.4	1117.4 ± 104.3
10/10	40.0 ± 1.54	226.2 ± 30.05	1025.9 ± 102.7	1124.3 ± 98.8
5/15	47.9 ± 1.27	254.3 ± 32.41	935.8 ± 90.7	1199.3 ± 101.4

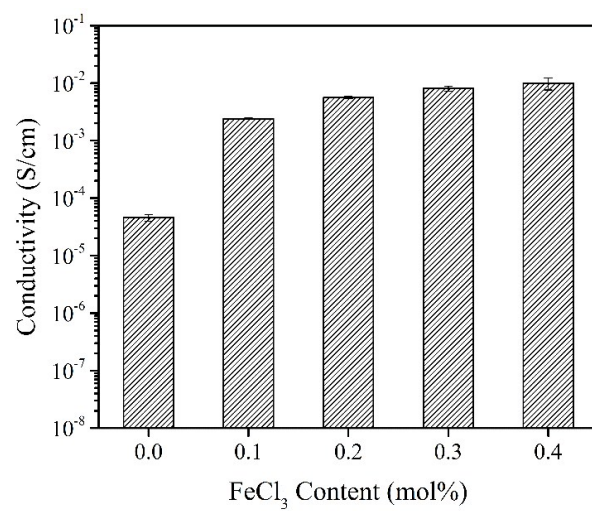


Figure S6. Conductivity of PAA/CS/GO gel with different FeCl₃ content.

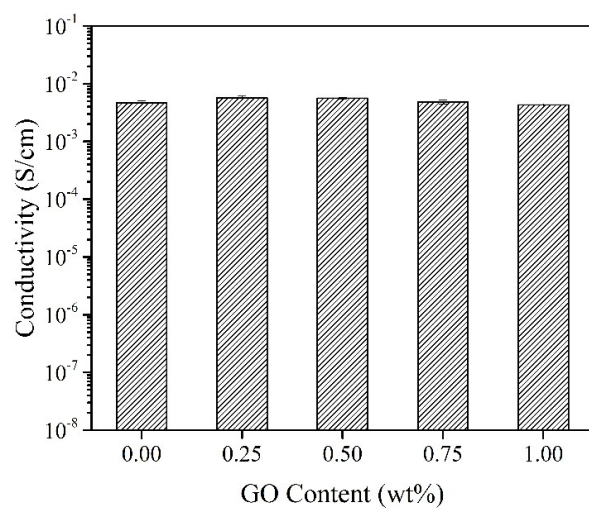


Figure S7. Conductivity of PAA/CS/GO gel with different GO content.

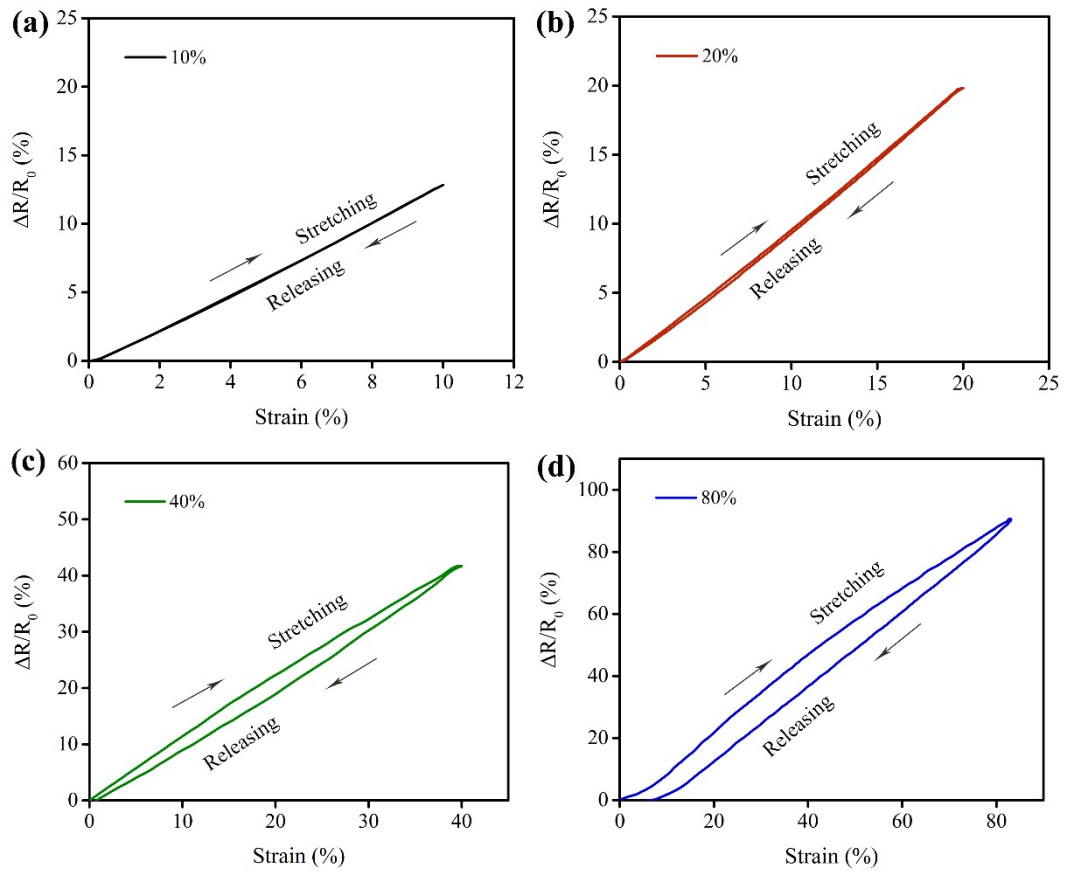


Figure S8. Hysteresis behavior of strain sensor at strain of 10%, 40% and 80%.

Table S4. The comparison between our strain sensor and exiting strain sensor.

Reference	Minimum detection strain	Response time	GF in linear region
Ref.11	0.3%	--	<2.0
Ref. 20	--	31 ms	~0.71
Ref. 28	--	230 ms	2.143
Ref.36	0.1%	156 ms	0.6
Ref. 37	0.1%	--	1.62
Ref.38	0.5%	--	0.7
Ref.39	0.3%	200 ms	~1.5
This work	0.25%	40 ms	1.138

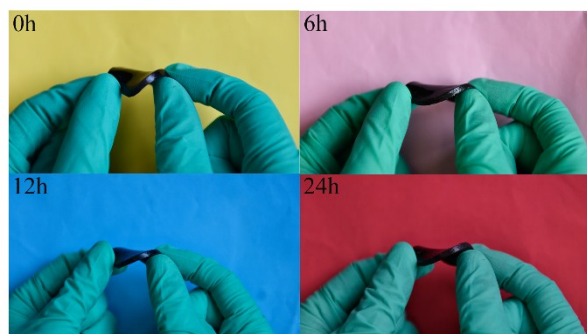


Figure S9. Photographs of the PAA/CS/GO/Gly gel that were twisted after storage at - 20 °C for different times.

The tensile curves of the PAA/CS/GO/Gly gel remained substantially the same even after storing at $-20\text{ }^{\circ}\text{C}$ for 24 h. It indicated that the PAA/CS/GO/Gly gel had excellent anti-freezing property and could be flexible and stretchable even under low temperature environment.

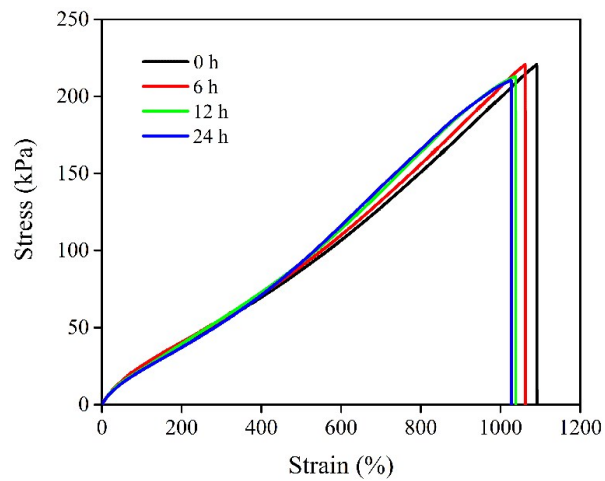


Figure S10. The tensile curves of PAA/CS/GO/Gly gel after storing at $-20\text{ }^{\circ}\text{C}$ for different time.

In order to further study the anti-freezing performance, dynamic temperature sweep measurements of gels were performed (Figure S11). Apparently, the storage modulus (G' , filled symbols) and loss modulus (G'' , unfilled symbols) of the PAA/CS/GO gel showed a significant increase when the temperature decreased from 0 to $-20\text{ }^{\circ}\text{C}$ due to the freezing of water inside PAA/CS/GO gel in this temperature range. On the contrast, the PAA/CS/GO/Gly gel showed stable elasticity under subzero temperature, indicating significant anti-freezing performance. Moreover, the storage modulus and loss modulus of gels gradually decreased with the temperature increased, indicating that the molecular chains of all gels were relaxed.

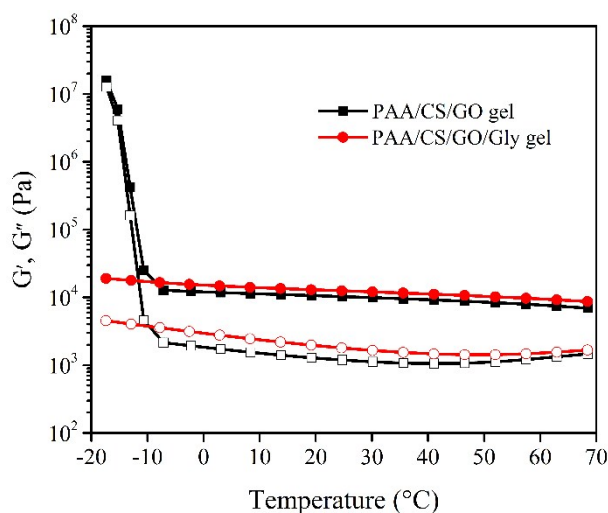


Figure S11. Dynamic temperature-sweep measurements of PAA/CS/GO gel and PAA/CS/GO/Gly gel.

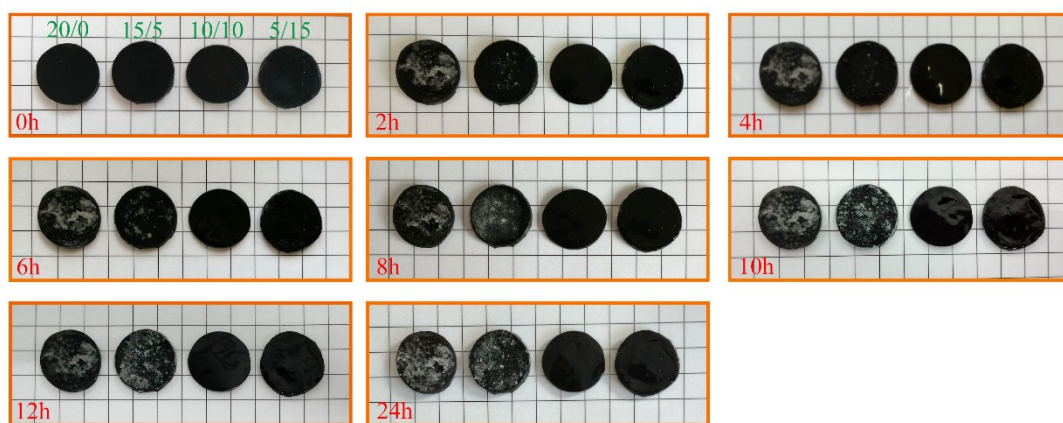


Figure S12. The photos of the PAA/CS/GO/Gly gel with different ration of H₂O and glycerol after storing at -20 °C for different time.

The effect of the ratio of H₂O and glycerol on the crystallization temperature of PAA/CS/GO/Gly gel was measured. As shown in Figure S13, the crystallization peak shifted toward to lower temperature as the glycerol content increased, indicating the addition of glycerol played a key role in improving the anti-freezing property of PAA/CS/GO/Gly gel. For the PAA/CS/GO/Gly gel at the ratio of H₂O and glycerol of 5/15, since the test temperature was limited, no crystallization peak appears in the range of -70, so it also proved that the more glycerol content, the lower the crystallization temperature.

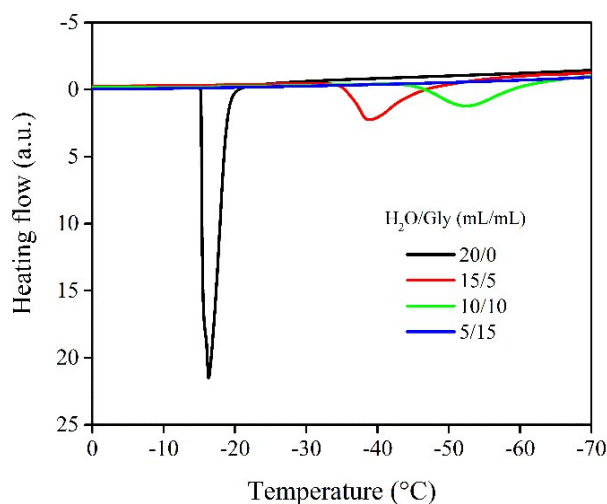


Figure S13. The DSC curves of PAA/CS/GO/Gly gel with different ratio of H₂O and glycerol.

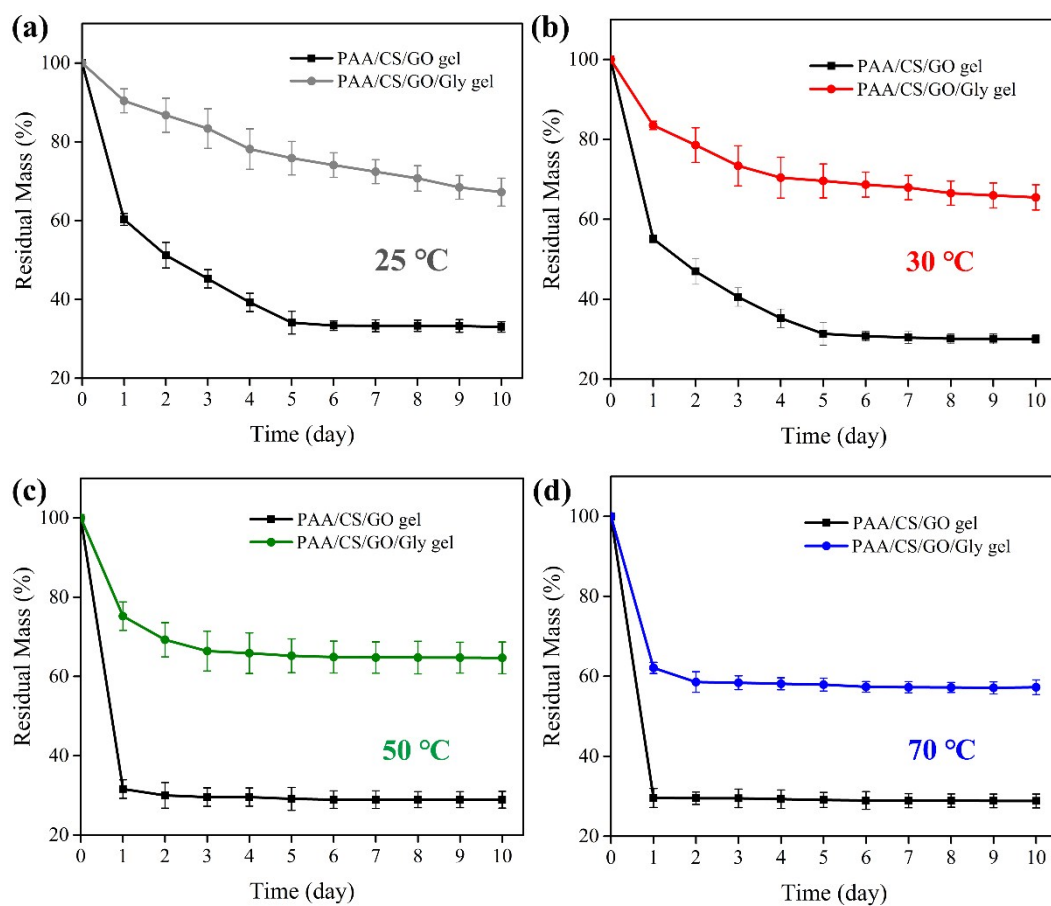


Figure S14. The residual mass for PAA/CS/GO gel and PAA/CS/GO/Gly gel at different temperature and time.

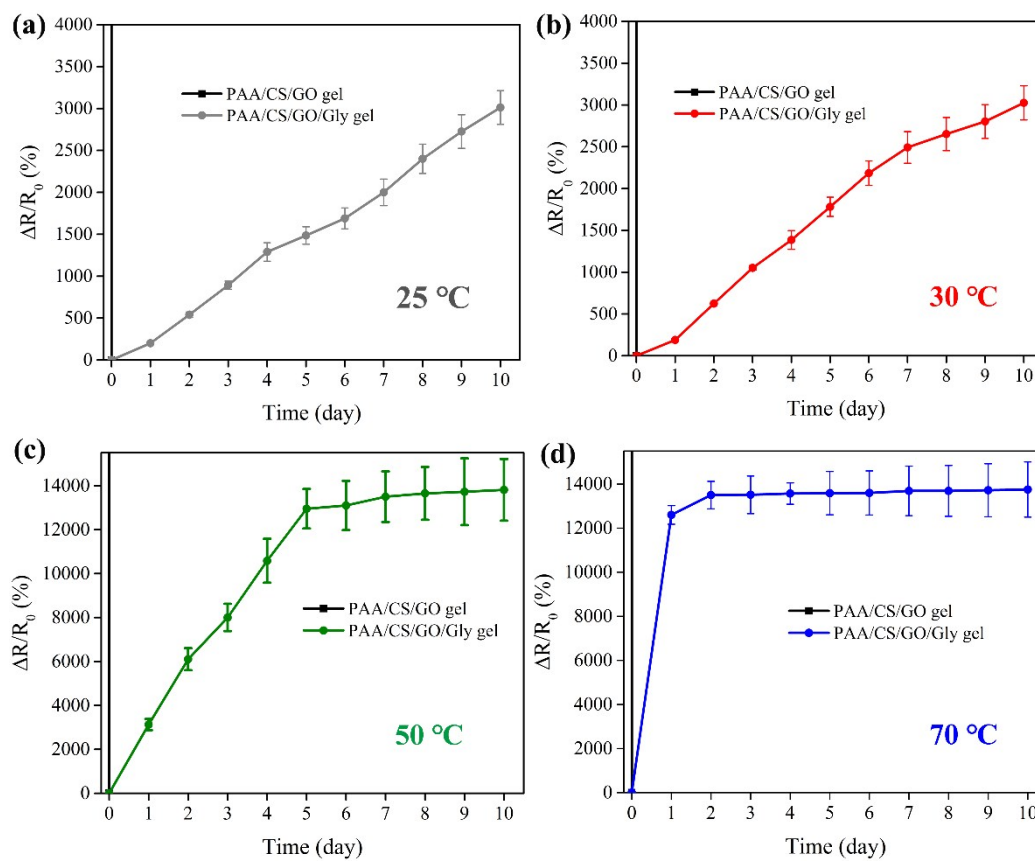


Figure S15. The resistance variation for PAA/CS/GO gel and PAA/CS/GO/Gly gel at different temperature and time.

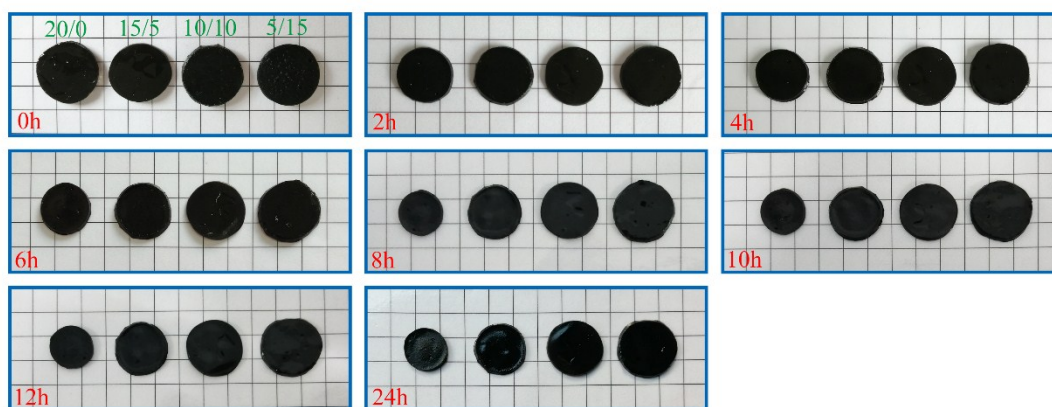


Figure S16. The photos of the PAA/CS/GO/Gly gel with different ration of H₂O and glycerol after storing at 70 °C for different time.

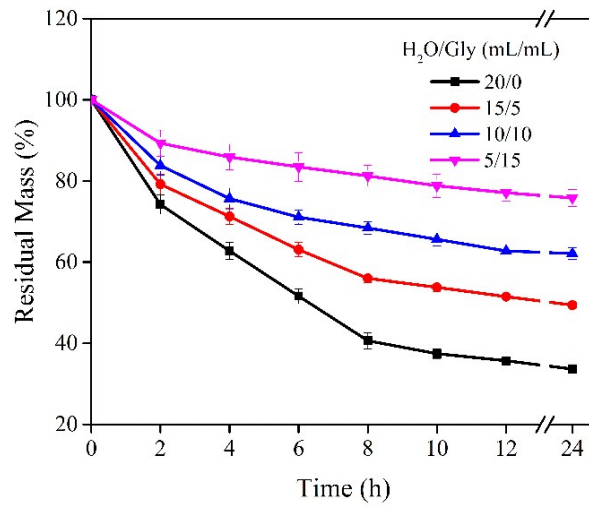


Figure S17. The water loss curves for PAA/CS/GO/Gly gel with different ratio of H₂O and Gly during storing at 70 °C for different time.

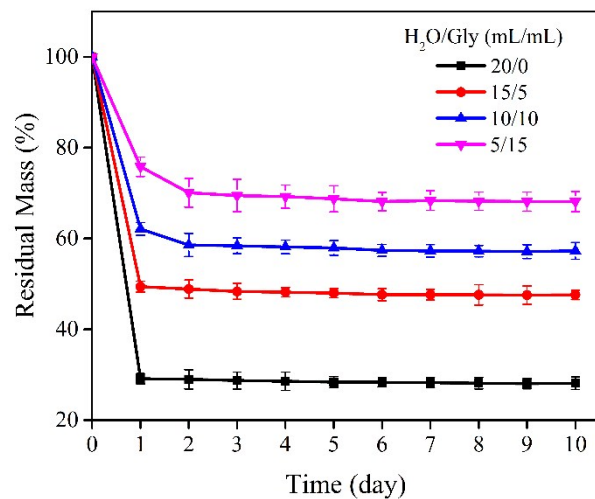


Figure S18. The water loss curves for PAA/CS/GO/Gly gel with different ratio of H₂O and Gly during storing at 70 °C for ten days.

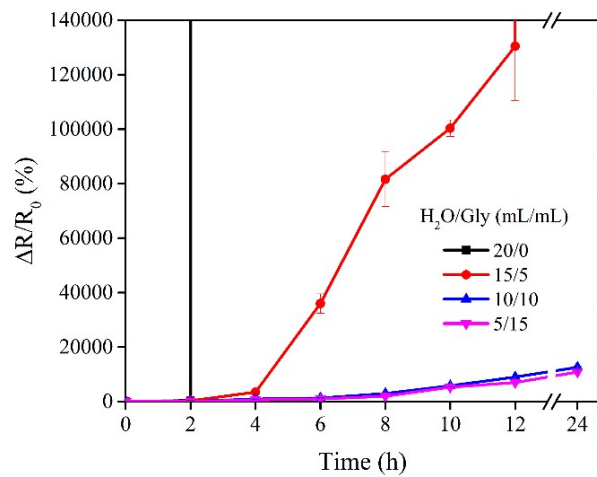


Figure S19. The resistance variation for PAA/CS/GO/Gly gel with different ratio of H₂O and Gly during storing at 70 °C for different time.

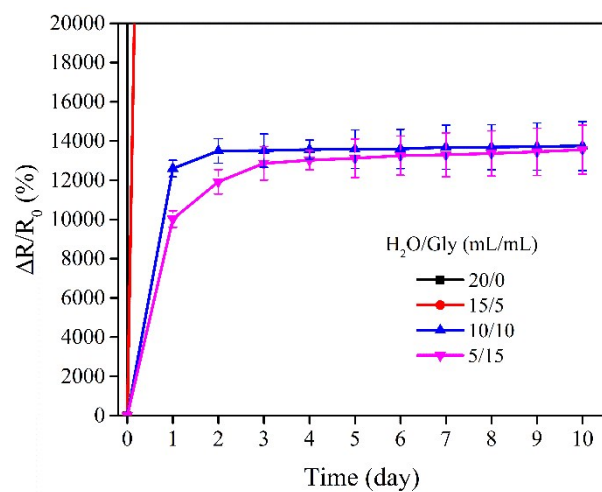


Figure S20. The resistance variation for PAA/CS/GO/Gly gel with different ratio of H₂O and Gly during storing at 70 °C for ten days.

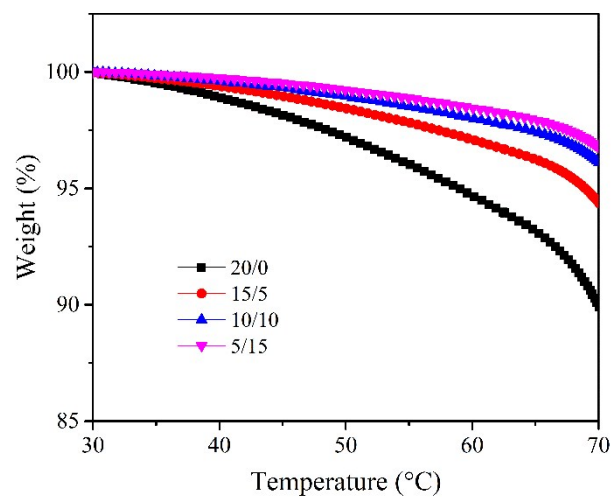


Figure S21. The TGA curves of PAA/CS/GO/Gly gel with different ratio of H₂O and Gly at temperature range from 30°C to 70 °C.

In order to evaluate the self-healing properties of PAA/CS/GO/Gly gel, rheological recovery tests were performed (Figure S22). Firstly, a shear strain sweep test was conducted on PAA/CS/GO/Gly gel. Under small amplitude strain, the G' was always larger than G'' in a linear region, indicating elastic (gel-like) behavior of gels. However, as the shear strains increased, the G' decreased gradually while the G'' increased. When the shear strain further increased, the G'' gradually exceeded the G' , meaning the transition behavior from solid (gel) to viscous fluid (sol). The gel-sol transition point where storage modulus G' and loss modulus G'' curves intersected was occurred at the shear strain of 52%. Based on the shear strain amplitude sweep results, the continuous step shear strain tests were performed to measure the rheology recovery behavior of the PAA/CS/GO/Gly gel. As shown in Figure S22b, the large strains (100%) for maintaining 100 s and the small strain (1%) for maintaining 200 s were alternatively applied on PAA/CS/GO/Gly gel. It was clearly that the sample exhibited a sol state at a large strain, then the sample gradually recovered to a gel state after the strain was declining, suggesting that the gel network exhibited rapid recovery when the it was subject to oscillatory shear strain.

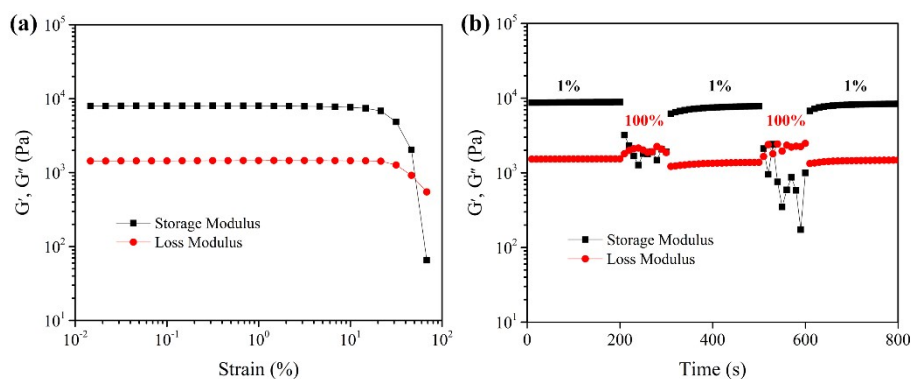


Figure S22. a) storage modulus (G') and loss modulus (G'') of PAA/CS/GO/Gly gel; b) cyclic G' and G'' values of PAA/CS/GO/Gly gel at a strain of 100% with resting time of 100 s and a strain of 1% with resting time of 200 s.